Pergamon

Computers & Structures Vol. 50, No. 1, pp. 47–57, 1994

0045-7949/94 $6.00 + 0.00

NONLINEAR DYNAMIC ANALYSIS OF MULTIPLE BUILDING BASE ISOLATED STRUCTURES

P. C. TSOPELAS, S. NAGARAJAIAH, M. C. CONSTANTINOU and A. M. REINHORN
Department of Civil Engineering, State University of New York at Buffalo, Buffalo, NY 14260, U.S.A.

(*Received* 28 *August* 1992)

Abstract—In long base isolated buildings the superstructure may consist of several parts separated by narrow thermal expansion joints. In such cases, neighboring bearings which support adjacent buildings are connected together at their top so that they form a common isolation and prevent impact at the isolation level. The analysis of such buildings constitutes the problem of a multiple base-isolated structure with a common basemat and isolation system. This situation can not be analyzed with the existing algorithms which are capable of analyzing only a single base-isolated structure. The torsional characteristics of the combined system are different than those of individual buildings on individual isolation systems. Hence, the combined system of several buildings on a common isolation system needs to be analyzed in its entirety rather than analyzing each building with its isolation system separately. In this paper an analytical model and an algorithm to analyze multiple buildings on a common isolation system are presented. Verification of the accuracy of the algorithm by comparison with results obtained using a general purpose finite element program are presented. A multiple building base-isolated structure is analyzed and the results are used to demonstrate the importance of analyzing the combined system as against analyzing individual buildings.

INTRODUCTION

In the last few years, seismic isolation has become an accepted design technique for buildings and bridges [1–3]. There are two basic types of isolation systems, one typified by elastomeric bearings and the other typified by sliding bearings. Furthermore, combinations of sliding and elastomeric systems and helical steel spring–viscous damper systems have found application. Several applications of isolation systems in buildings and bridges have been reported [1–4].

Most isolation systems exhibit strong nonlinear behavior. Their force–deflection properties depend on the axial load, bilateral load and rate of loading. Under these conditions, the recently developed requirements for isolated structures [5] require that dynamic time history analysis be performed for the isolated structure. The analysis should account for the spatial distribution of isolator units and the aforementioned force–deflection properties.

Existing general purpose nonlinear dynamic analysis computer programs like DRAIN-2D [6] and ANSR [7] can be used in the dynamic analysis of base-isolated structures. These programs are limited to elements exhibiting bilinear hysteretic behavior and can not accurately model sliding bearings.

Special purpose computer programs for the analysis of base-isolated structures have been developed. Computer program NPAD [8] has plasticity based nonlinear elements that can be used to model certain types of elastomeric bearings. Program 3D-BASIS [9, 10] utilizes viscoplasticity-based elements that can model a wide range of isolation devices, including elastomeric and sliding bearings. Both programs represent the superstructure by a condensed, three-degrees-of-freedom per floor model. They are limited to the case of a single building on the top of a rigid basemat with the isolation system below. A situation in which the aforementioned programs can not be used is that of multiple buildings on a common isolation basemat with the isolation system below. This situation occurs in long base-isolated buildings in which the superstructure consists of several buildings separated by thermal expansion joints. However, all neighboring bearings supporting adjacent buildings are connected together at their top, forming a common isolation system. This results in a complex of several buildings on a common isolation system. This type of construction prevents impact of the adjacent parts at the isolation basemat level.

The torsional characteristics of the combined system may be significantly different than those of the individual parts. The distance of corner bearings from the center of resistance of the combined system is much larger than that of the individual parts when unconnected. Thus when the combined system is set into torsional motion, the corner bearings may experience inelastic deformations much earlier than when the individual parts are not connected together. Furthermore, the motion experienced by each of the various parts of the combined system is different. This coupled with the possibility of significantly

different dynamic characteristics of each of the buildings above the common basemat may result in out-of-phase motion with possible impact of adjacent parts above the basemat.

To evaluate these possible effects it is necessary to analyze the complete system. Analysis of the individual parts as being unconnected from the rest may result in underestimation of the forces and displacements experienced by the system and may give insufficient information for assessing the possibility of impact of adjacent parts.

This paper presents the development of an analytical model for analyzing multiple buildings on a common isolation system. The buildings are modeled as elastic frame–shear wall structures. The superstructure parts and the common base are modeled with three degrees of freedom attached to the center of mass of each floor and base. The base and floors are assumed to be rigid diaphragms. The isolation system may include elastomeric, sliding bearings, and other hysteretic devices and dampers. The isolators are modeled by a discrete model which can represent the nonlinear biaxial characteristics of the isolators. The algorithm has been implemented in the computer program 3D-BASIS-M [11].

Comparisons with results obtained using the general purpose finite element program ANSR [7] are presented for verification of the developed algorithm. The results from the analysis of a multiple building base-isolated structure are used to demonstrate the significance of the aforementioned effects and the usefulness of the algorithm.

SUPERSTRUCTURE AND ISOLATION SYSTEM CONFIGURATION

In this section the overall configuration of multiple building base-isolated structures is described. The superstructure and the isolation system modeling are presented. Figure 1 shows a number of buildings on a common isolation system and basemat. The degrees of freedom are attached to the center of mass of the floors and base. A global reference axis is attached to the center of mass of the base. The coordinates of the center of mass of each floor of each building are measured with respect to this global reference axis. The center of resistance of each floor may be located arbitrarily with respect to the center of mass of the floor (see Fig. 1). Displacements and rotations of each floor are measured with respect to the base, whereas those of the base are measured with respect to the ground.

SUPERSTRUCTURE MODELING

The superstructure is assumed to remain elastic at all times. Coupled lateral–torsional response is accounted for by maintaining three degrees of freedom per floor, that is two translational and one rotational degree of freedom (see Fig. 1). The floors and base are considered to be rigid diaphragms. A modal representation is chosen for the three-dimensional superstructure so that the dynamic characteristics of the various buildings, determined in their fixed base condition by computer programs like ETABS [12], can be utilized in the analysis. This modal data is integrated into the

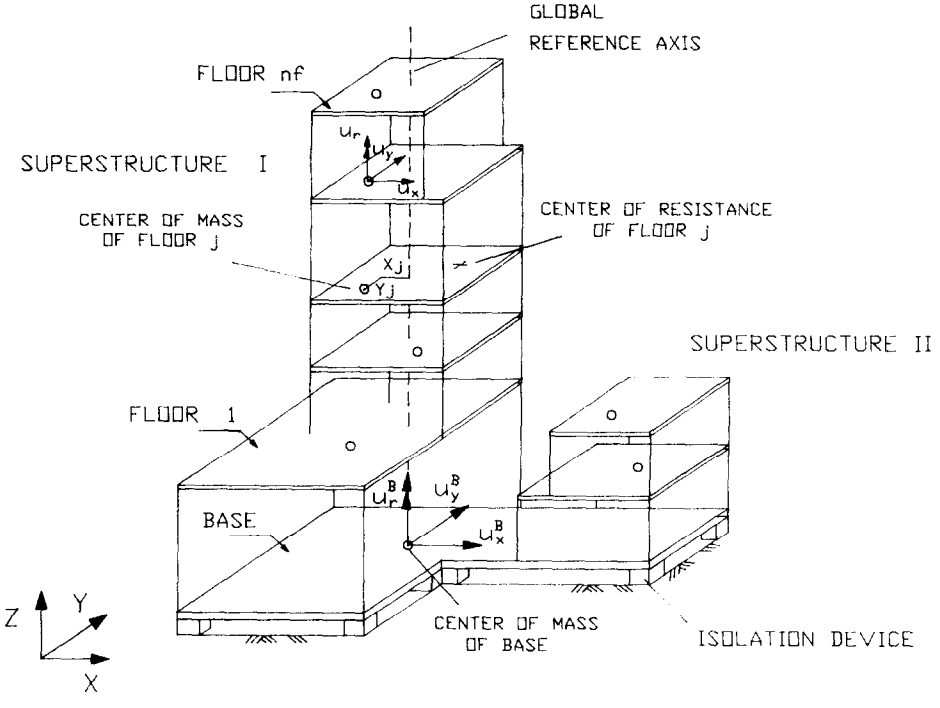

Fig. 1. Multiple building base-isolated structure.

global model which includes both the superstructure and the isolation system. In this way, the extensibility of the vertical elements, arbitrary location of the center of mass and floor flexibility may be implicitly accounted for. The data needed for the dynamic analysis are the mass and the mass moment of inertia of each floor, frequencies, mode shapes and associated damping ratios for the chosen number of modes.

ISOLATION SYSTEM MODELING

The isolation system is modeled with spatial distribution and explicit nonlinear force–displacement characteristics of individual isolation devices. The isolation devices are considered rigid in the vertical direction and individual devices are assumed to have negligible resistance to torsion.

Isolation elements are primarily elastomeric bearings, which may be represented by models with smooth bilinear characteristics and sliding bearings, which may be represented by models with rigid-plastic characteristics. The uniaxial and biaxial behavior of elastomeric bearings has been modeled by Japanese researchers [13] using a multiple spring model and by Way and Jeng [8] using a plasticity-based nonlinear model. Mostaghel and Khodaverdian [14] and Su *et al.* [15] have used the conventional method of keeping track of stick-slip conditions for representing the uniaxial behavior of sliding bearings. The authors [9, 10] have used a viscoplasticity-based model for representing biaxial and uniaxial behavior of both elastomeric and sliding bearings.

The model used in the formulation of this paper is capable of modeling both uniaxial and biaxial behavior of elastomeric and sliding bearings. The model for sliding bearings can account for the variation of the coefficient of friction with velocity of sliding and bearing pressure which was observed in Teflon sliding bearings [16]. The model for elastomeric bearings can model either lead–rubber bearings [3] or high damping bearings [1]. First the biaxial model and then the uniaxial model which is a particular case of the biaxial model are described.

Biaxial model for elastomeric bearings and steel dampers

The forces along the orthogonal directions, which are mobilized during motion of an elastomeric bearing or steel damper, are described by

$$F_x = \alpha \frac{F^y}{Y} U_x + (1-\alpha) F^y Z_x \tag{1a}$$

$$F_y = \alpha \frac{F^y}{Y} U_y + (1-\alpha) F^y Z_y \tag{1b}$$

in which, α is the post-yielding to the pre-yielding stiffness ratio, F^y is the yield force and Y is the yield displacement. Z_x and Z_y are dimensionless variables governed by the following system of differential equations which was proposed by Park *et al.* [17]

$$\begin{Bmatrix} \dot{Z}_x & Y \\ \dot{Z}_y & Y \end{Bmatrix} = \begin{Bmatrix} A & \dot{U}_x \\ A & \dot{U}_y \end{Bmatrix} - \begin{pmatrix} Z_x^2(\gamma\ \mathrm{Sgn}(\dot{U}_x Z_x) + \beta) & Z_x Z_y(\gamma\ \mathrm{Sgn}(\dot{U}_y Z_y) + \beta) \\ Z_x Z_y(\gamma\ \mathrm{Sgn}(\dot{U}_x Z_x) + \beta) & Z_y^2(\gamma\ \mathrm{Sgn}(\dot{U}_y Z_y) + \beta) \end{pmatrix} \begin{Bmatrix} \dot{U}_x \\ \dot{U}_y \end{Bmatrix} \tag{2}$$

in which A, γ and β are dimensionless quantities that control the shape of the hyperesis loop. Furthermore, U_x, U_y and $\dot{U}_x$, $\dot{U}_y$ are the displacements and velocities that occur at the isolation device, respectively.

Constantinou *et al.* [16] have shown that the interaction curve between the forces in the two directions is circular only when the condition $A/(\beta+\gamma) = 1$ is satisfied. In particular, $A = 1$ and $\beta = 0.1$ and $\gamma = 0.9$ are used in the present study.

Biaxial model for sliding bearings

For sliding bearings, the mobilized forces are described by the following equations [16]

$$F_x = \mu_s N Z_x \tag{3a}$$

$$F_y = \mu_s N Z_y \tag{3b}$$

in which N is the vertical load carried by the bearing and μ_s is the coefficient of sliding friction which depends on the bearing pressure, direction of motion and the instantaneous velocity of sliding $\dot{U}$

$$\dot{U} = (\dot{U}_x^2 + \dot{U}_y^2)^{1/2}. \tag{4}$$

The conditions of separation and reattachment and biaxial interaction are accounted for by variables Z_x and Z_y in eqn (2). The coefficient of sliding friction is modeled by the following equation suggested by Constantinou *et al.* [16]

$$\mu_s = f_{\max} - \Delta f \exp(-a|\dot{U}|) \tag{5}$$

in which, $f_{\max}$ is the maximum value of the coefficient of friction and Δf is the difference between the maximum and minimum (at $\dot{U} = 0$) values of the coefficient of friction. Furthermore, a is a parameter which controls the variation of the coefficient of friction with velocity of sliding. Values of parameters $f_{\max}$, Δf and a for interfaces used in sliding bearings have been reported in Constantinou *et al.* [16] and Mokha *et al.* [18, 19]. In general, parameters $f_{\max}$, Δf and a are functions of bearing pressure and direction of motion even though the dependency on the latter is usually not important.

Uniaxial model for elastomeric bearings and sliding bearings

The biaxial interaction achieved in the models of eqns (1)–(5) may be disregarded by replacing the

off-diagonal elements in eqn (2) by zeros. This leads to two uniaxial independent elements having either sliding or smooth hysteretic behavior in the two orthogonal directions. The model for sliding bearings has been verified for both unidirectional and bidirectional motions. Experimental studies, conducted by Constantinou *et al.* [16] and Mokha *et al.* [19], verified the validity of the model used herein. Furthermore, analytical studies reported in Mokha *et al.* [19] demonstrated that the neglect of biaxial interaction in isolation bearings may lead to considerable underestimation of the isolation system displacement response.

ANALYTICAL MODEL AND EQUATIONS OF MOTION

A typical multiple building base-isolated structure is shown in Fig. 1. The equation of motion, governing a typical superstructure building (i) with total number of floors (nf^i), is written as

$$\mathbf{M}^i\ddot{\mathbf{u}}^i + \mathbf{C}^i\dot{\mathbf{u}}^i + \mathbf{K}^i\mathbf{u}^i = -\mathbf{M}^i\mathbf{r}^i(\ddot{\mathbf{u}}_b + \ddot{\mathbf{u}}_g) \tag{6}$$

where $\mathbf{M}^i$, $\mathbf{C}^i$, $\mathbf{K}^i$ are the mass, damping and stiffness matrices of the typical building (matrix dimensions $3nf^i \times 3nf^i$) and $\mathbf{r}^i$ is a rectangular matrix with dimensions $3nf^i \times 3$ which transforms the base, $\ddot{\mathbf{u}}_b$, and ground, $\ddot{\mathbf{u}}_g$, acceleration vectors from the center of mass of the base to the center of mass of each floor for the typical building. Furthermore, $\ddot{\mathbf{u}}^i$, $\dot{\mathbf{u}}^i$, $\mathbf{u}^i$ are, respectively, the vectors of acceleration, velocity and displacement relative to the base.

Combining the equations of motion from every superstructure building, (total number of superstructure buildings (ns)), the following equation is obtained

$$\mathbf{M}\ddot{\mathbf{u}} + \mathbf{C}\dot{\mathbf{u}} + \mathbf{K}\mathbf{u} = -\mathbf{M}\mathbf{R}(\ddot{\mathbf{u}}_b + \ddot{\mathbf{u}}_g) \tag{7}$$

where

$$\mathbf{M} = \begin{bmatrix} \mathbf{M}^1 & & \\ & \mathbf{M}^i & \\ & & \mathbf{M}^{ns} \end{bmatrix}_{\left(\sum_{i=1}^{ns} 3nf^i \times \sum_{i=1}^{ns} 3nf^i\right)} \tag{8}$$

$$\mathbf{C} = \begin{bmatrix} \mathbf{C}^1 & & \\ & \mathbf{C}^i & \\ & & \mathbf{C}^{ns} \end{bmatrix}_{\left(\sum_{i=1}^{ns} 3nf^i \times \sum_{i=1}^{ns} 3nf^i\right)} \tag{9}$$

$$\mathbf{K} = \begin{bmatrix} \mathbf{K}^1 & & \\ & \mathbf{K}^i & \\ & & \mathbf{K}^{ns} \end{bmatrix}_{\left(\sum_{i=1}^{ns} 3nf^i \times \sum_{i=1}^{ns} 3nf^i\right)} \tag{10}$$

$$\ddot{\mathbf{u}} = \begin{Bmatrix} \ddot{\mathbf{u}}^1 \\ \ddot{\mathbf{u}}^i \\ \ddot{\mathbf{u}}^{ns} \end{Bmatrix}_{\left(\sum_{i=1}^{ns} 3nf^i \times 1\right)} \tag{11}$$

$$\mathbf{R} = \begin{bmatrix} \mathbf{r}^1 \\ \mathbf{r}^i \\ \mathbf{r}^{ns} \end{bmatrix}_{\left(\sum_{i=1}^{ns} 3nf^i \times 3\right)} \tag{12}$$

The submatrix $\mathbf{r}^i$ of the typical building (i) has the form

$$\mathbf{r}^i = \begin{bmatrix} \bar{\mathbf{R}}^{nf^i} \\ \bar{\mathbf{R}}^j \\ \bar{\mathbf{R}}^1 \end{bmatrix} \tag{13}$$

with each one of the submatrices $\bar{\mathbf{R}}^j$ given by

$$\bar{\mathbf{R}}^j = \begin{bmatrix} 1 & 0 & -y_j \\ 0 & 1 & x_j \\ 0 & 0 & 1 \end{bmatrix}, \tag{14}$$

where x_j, y_j are the distances in X and Y directions of the center of mass of the jth floor of the ith superstructure building from the center of mass of the base (measured with respect to the global reference axis, see Fig. 1). The equations of dynamic equilibrium of the base are

$$\mathbf{R}^T\mathbf{M}[\ddot{\mathbf{u}} + \mathbf{R}(\ddot{\mathbf{u}}_b + \ddot{\mathbf{u}}_g)] + \mathbf{M}_b(\ddot{\mathbf{u}}_b + \ddot{\mathbf{u}}_g) + \mathbf{C}_b\dot{\mathbf{u}}_b + \mathbf{K}_b\mathbf{u}_b + \mathbf{f}_N = 0, \tag{15}$$

where $\dot{\mathbf{u}}_b$, and $\mathbf{u}_b$ are (3×1) vectors representing the base velocity and displacement with respect to the ground, respectively. Furthermore, $\mathbf{M}_b$, $\mathbf{C}_b$ and $\mathbf{K}_b$ are, respectively, the mass matrix of the base, the resultant damping matrix and the resultant stiffness matrix of any linear viscous elements and of any linear elastic elements of the isolation system. Vector $\mathbf{f}_N$ embodies the forces mobilized in the nonlinear elements of the isolation system.

Modal reduction is employed for the purpose of allowing, as an option, the use of a reduced number of degrees of freedom in the dynamic analysis. The transformation leading to modal reduction is

$$\mathbf{u}^i = \boldsymbol{\Phi}^i\mathbf{y}^i, \tag{16}$$

where $\boldsymbol{\Phi}^i$ is a matrix containing in its columns the undamped eigenvectors (mode shapes) of building i. The matrix is orthogonal so that $\boldsymbol{\Phi}^{iT}\mathbf{M}^i\boldsymbol{\Phi}^i$ is an identity matrix. Matrix $\boldsymbol{\Phi}^i$ has dimensions $(3nf^i \times ne^i)$, where ne^i is the number of eigenvectors of building i retained in the analysis. Furthermore, $\mathbf{y}^i$ is the modal displacement vector of building i.

Combining eqns (6)–(16), the following system of equations is derived

$$\begin{pmatrix} \mathbf{I} & \boldsymbol{\Phi}^T\mathbf{M}\mathbf{R} \\ \mathbf{R}^T\mathbf{M}\boldsymbol{\Phi}^T & \mathbf{R}^T\mathbf{M}\mathbf{R} + \mathbf{M}_b \end{pmatrix}_{(m_b+3)\times(m_b+3)} \begin{Bmatrix} \ddot{\mathbf{y}} \\ \ddot{\mathbf{u}}_b \end{Bmatrix}_{(m_b+3)\times 1} + \begin{pmatrix} 2\xi\boldsymbol{\omega} & \mathbf{0} \\ \mathbf{0} & \mathbf{C}_b \end{pmatrix}_{(m_b+3)\times(m_b+3)} \begin{Bmatrix} \dot{\mathbf{y}} \\ \dot{\mathbf{u}}_b \end{Bmatrix}_{(m_b+3)\times 1} + \begin{pmatrix} \boldsymbol{\omega}^2 & \mathbf{0} \\ \mathbf{0} & \mathbf{K}_b \end{pmatrix}_{(m_b+3)\times(m_b+3)} \begin{Bmatrix} \mathbf{y} \\ \mathbf{u}_b \end{Bmatrix}_{(m_b+3)\times 1} + \begin{Bmatrix} \mathbf{0} \\ \mathbf{f}_N \end{Bmatrix}_{(m_b+3)\times 1} = -\begin{pmatrix} \boldsymbol{\Phi}^T\mathbf{M}\mathbf{R} \\ \mathbf{R}^T\mathbf{M}\mathbf{R} + \mathbf{M}_b \end{pmatrix}_{(m_b+3)\times 3} \ddot{\mathbf{u}}_{g(3\times 1)} \tag{17}$$

in which m_b is the total number of eigenvectors, from all buildings, which is retained in the analysis. Furthermore, matrices $\boldsymbol{\xi\omega}$ and $\boldsymbol{\omega}^2$ are diagonal with dimensions ($m_b \times m_b$) and contain, respectively, the product of modal damping, ξ, and frequency, ω, and frequency squared, ω^2, of all the modes (from all buildings) which are retained in the analysis. Matrices **I** and **0** denote identity and null matrices, respectively. Furthermore, $\boldsymbol{\Phi}$ is matrix of dimensions ($\Sigma_{i=1}^{ns} 3nf^i \times \Sigma_{i=1}^{ns} 3ne^i$) having along its diagonal the matrices $\boldsymbol{\Phi}^i$.

Equation (17) is the system of the governing differential equations of motion which has to be solved together with eqns (2) and (1) or (3) depending on the type of nonlinearity in the isolation system.

Method of solution and solution algorithm

The solution of the system of eqns (1)–(3) and (17) is obtained through an incremental analysis procedure involving two stages.

(i) Solution of the equations of motion (17) using the unconditionally stable Newmark's average-acceleration method [20].

(ii) Solution of differential equations (1)–(3), governing the nonlinear behavior of the isolation elements, using an unconditionally stable semi-implicit Runge–Kutta method [21], which is suitable for stiff differential equations. The solution algorithm is developed by Nagarajaiah *et al.* [9] and implemented in computer program 3D-BASIS [9] is adopted. The interested reader is referred to [9] for details.

NUMERICAL VERIFICATION

Many existing computer programs can be used to model base-isolated structures when the isolation system consists of elements exhibiting bilinear hysteretic behavior. Examples of these computer programs are DRAIN-2D [6] and ANSR [7], among others. All these programs are for general purpose nonlinear dynamic analysis. Furthermore, these programs can not accurately handle special devices used in base isolation, such as sliding bearings. Accordingly, the tools available to verify the presented algorithm are limited.

The dynamic response of the multiple building isolated structure of Fig. 2 is analyzed using computer programs 3D-BASIS-M and ANSR [7]. The superstructure consists of three one-story buildings placed on a rigid L-shaped base. Each building has plan dimensions L by L where $L = 12.2$ m and story height $H = 4.6$ m. The buildings are separated by a gap $S = 305$ mm. The weight of each building is $W = 1070$ kN. The center of mass coincides with the geometric center of each floor. However, the center of resistance of each building has an offset of 0.1 L from the center of mass in both directions, resulting in nonuniform distribution of stiffness as illustrated in Fig. 2. The total stiffness of each building in both lateral directions is equal to 47.6 kN/mm and the torsional stiffness at the center of mass is equal to 3547682 kN m. These properties result in the following fixed base periods of each building: $T_1 = 0.335$ sec, $T_2 = 0.299$ sec, and $T_3 = 0.274$ sec. In the analysis with 3D-BASIS-M, viscous damping of 2% of critical was assumed in each vibration mode of each superstructure building. In the ANSR model, an appropriate mass proportional damping coefficient was used to simulate the damping considered in the 3D-BASIS-M model. Furthermore, in the ANSR model the floor mass was represented by four equal

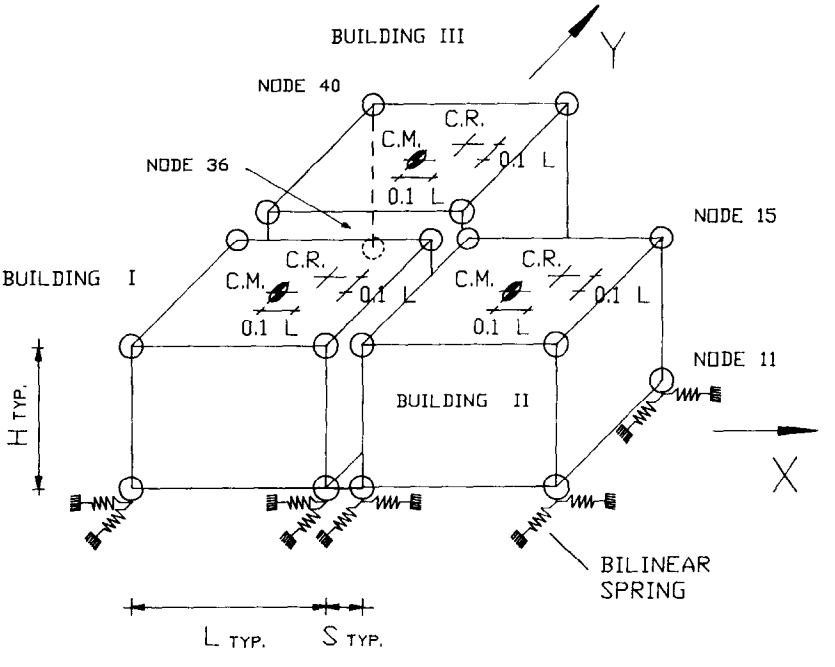

Fig. 2. ANSR model of multiple building base-isolated structure.

lumped masses placed at the four corners as shown in Fig. 2.

The isolation system is placed below the rigid L-shaped basemat and consists of twelve isolation bearings (four below each building at the corners). The weight of the L-shaped basemat was assumed to be equal to that of the three buildings ($3 \times 1070 = 3210$ kN). In the ANSR model, the basemat mass is represented by twelve equal lumped masses, each one at the bottom of each column of the buildings as shown in Fig. 2.

Each isolation bearing has bilinear behavior which is modeled by two nonlinear springs placed along directions X and Y as illustrated in Fig. 2. Each of the bearings in buildings I and III has initial stiffness of 3.12 kN/mm, post-yielding stiffness of 0.48 kN/mm and yield force 29.36 kN. Each of the bearings in building II has initial stiffness of 1.89 kN/mm, post-yielding stiffness of 0.29 kN/mm and yield force of 17.79 kN. The uneven distribution of stiffness results in an eccentrically placed center of resistance in the common isolation system. Based on the initial bearing stiffnesses, the eccentricities are $e_x = 1270$ mm and $e_y = 635$ mm with respect to the center of mass of the common base. The eccentricities amount to 5% and 2.5% of the plan dimensions of the complex, respectively. It should be noted that the combined yield force of the bearings is 0.048 times the weight of the complex and that the ratio of combined initial stiffness to combined post-yielding stiffness of the bearings is 6.5. These parameters are typical of lead–rubber bearings [22]. Based on a 152 mm isolation system displacement (which represents the isolation system displacement for a ground motion having characteristics of Zone 4, Soil Type S2 spectrum according to the 1991 UBC [5]), the period of the isolated complex is equal to about 2 sec.

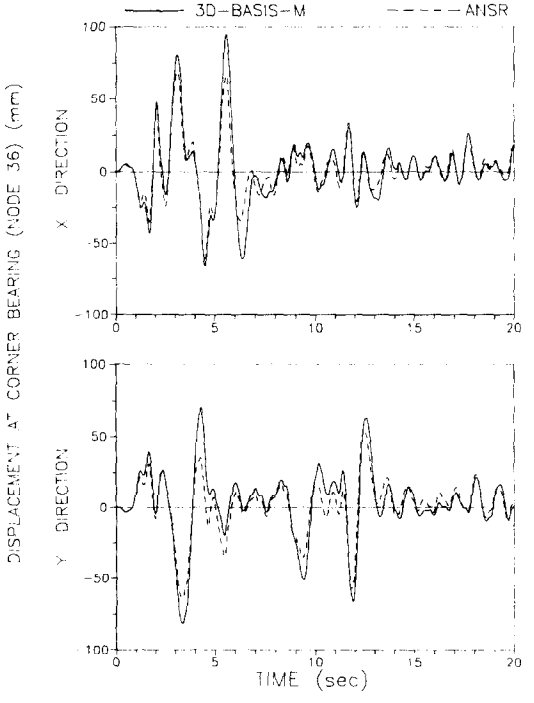

Fig. 3. Comparison of bearing displacements (Node 36) of multiple building isolated structure under bidirectional excitation.

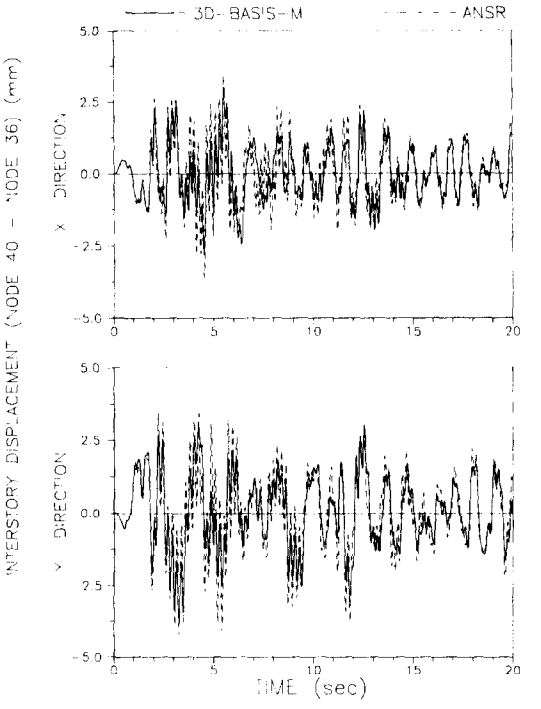

Fig. 4. Comparison of interstory displacements (Node 40–Node 36) of multiple building isolated structure under bidirectional excitation.

For modeling the complex (isolation system and superstructure) in ANSR, three dimensional truss elements were used. The masses were considered to be concentrated at the nodes as shown in Fig. 2. The in-plane rigidity of the floors was modeled using two linear truss elements having very large area and forming an X bracing. Diagonal truss elements with an appropriate value for area were used in each face of the buildings to simulate the lateral stiffness. Uniaxial bilinear elements were used to model the isolators in both 3D-BASIS-M and ANSR.

Bidirectional earthquake excitation was imposed with component S00E and S90W of the 1940 El Centro motion applied along directions X and Y, respectively. Computed corner bearing and interstory displacement histories by the two programs are compared in Figs 3 and 4. The responses compare well and the observed differences are attributed to differences in the two models describing the system.

A CASE STUDY

A hospital complex in Greece has been recently designed on a seismic isolation system consisting of lead–rubber bearings. The facility consists of five

buildings. Four of the buildings are to be seismically isolated with a common base and isolation system, and the fifth is to be constructed with a conventional fixed base. The design of the isolation system was originally based on analyses of the four isolated buildings assuming that were separately isolated and not connected at the isolation level. Subsequently, the entire isolated complex was analyzed using computer program 3D-BASIS-M. The differences in the response, which arise when one part (Part III) of the complex is analyzed as a separate isolated building and when it is analyzed considering the interaction with the other parts of the complex are presented in this section.

Description of facility

The hospital complex consists of four isolated six-story buildings (parts I–IV) and one non-isolated four-story building. The layout is shown in Fig. 5. The four isolated parts form a T-shape in plan with dimensions of approximately 76 m by 57 m. Part III has plan dimensions 10.8 m by 29.7 m. The four isolated buildings are separated by a 0.05 m thermal gap. The basemats of these four buildings are connected together at the isolation system level forming a large T-shaped isolation basemat.

The structural system consists of doubly reinforced concrete slabs supported by reinforced concrete columns and beams. The lateral force resisting system consists of concrete reinforced shear walls and infill brick shear panels with the slabs behaving as rigid diaphragms. The total seismic weight of the complex including superstructure (buildings) and basemat is $W_{tot} = 174.4$ MN. The seismic weight of part III (superstructure plus basemat) is $W_{III} = 37.6$ MN.

Table 1. Dynamic characteristics of parts of isolated complex

Building	Period T_1 (sec)	T_2 (sec)	T_3 (sec)
Part I	0.45	0.34	0.26
Part II	0.42	0.26	0.17
Part III	0.44	0.26	0.24
Part IV	0.34	0.30	0.20

The dynamic characteristics of each of the four superstructures of the complex are presented in Table 1 in terms of the periods of free vibration. These periods, the corresponding mode shapes and damping ratios (assumed to be 5% of critical in each mode) represented input to program 3D-BASIS-M. The periods and mode shapes were calculated in a detailed model of each part using program ETABS [12]. In the model, the stiffening effects of brick walls were included so that the calculated fundamental period of each part was consistent with empirical values. Each of the four superstructures could remain elastic for a structural shear force (first floor shear) of 0.23 times the seismic weight and an interstory drift of 0.2% of the story height.

Elastomeric bearings are placed at 153 locations under each column and at the ends of each shear wall. Thirty two of these bearings are placed below part III. Four types of bearings are used. Three of these types have cylindrical lead plug in the center

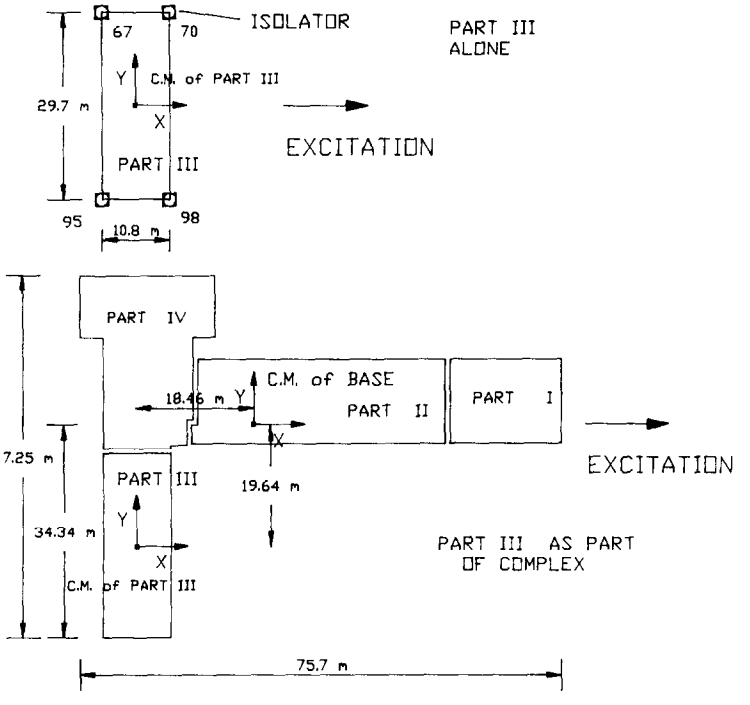

Fig. 5. Layout of isolated hospital complex.

Table 2. Properties of elastomeric bearings

	Bearing type			
	A	B	C	D
Dimensions (mm)	380 × 380	460 × 460	540 × 540	530 × 530
Bearing height (mm)	220	220	220	220
Lead core diameter (mm)	70	100	90	0
No. of rubber layers	13	13	13	13
Rubber layer thickness (mm)	9.5	9.5	9.5	9.5
Yield force (kN)	35.71	75.83	57.98	1.15
Yield displacement (mm)	5.23	7.06	4.35	1
Post yielding stiffness (kN/mm)	1.05	1.66	2.05	1.15
No. of bearings in part III	19	3	10	0
No. of bearings in complex	55	25	61	12

and one type is without lead core. The properties and the number of each type of bearing are presented in Table 2.

Nonlinear dynamic time history analyses of the entire complex and of part III along were performed using program 3D-BASIS-M. The 1971 San Fernando motion (Record No. 211, component NS) was scaled so that its 5% damped spectrum was compatible with the site specific response spectrum. Figure 6 shows the scaled ground acceleration record and

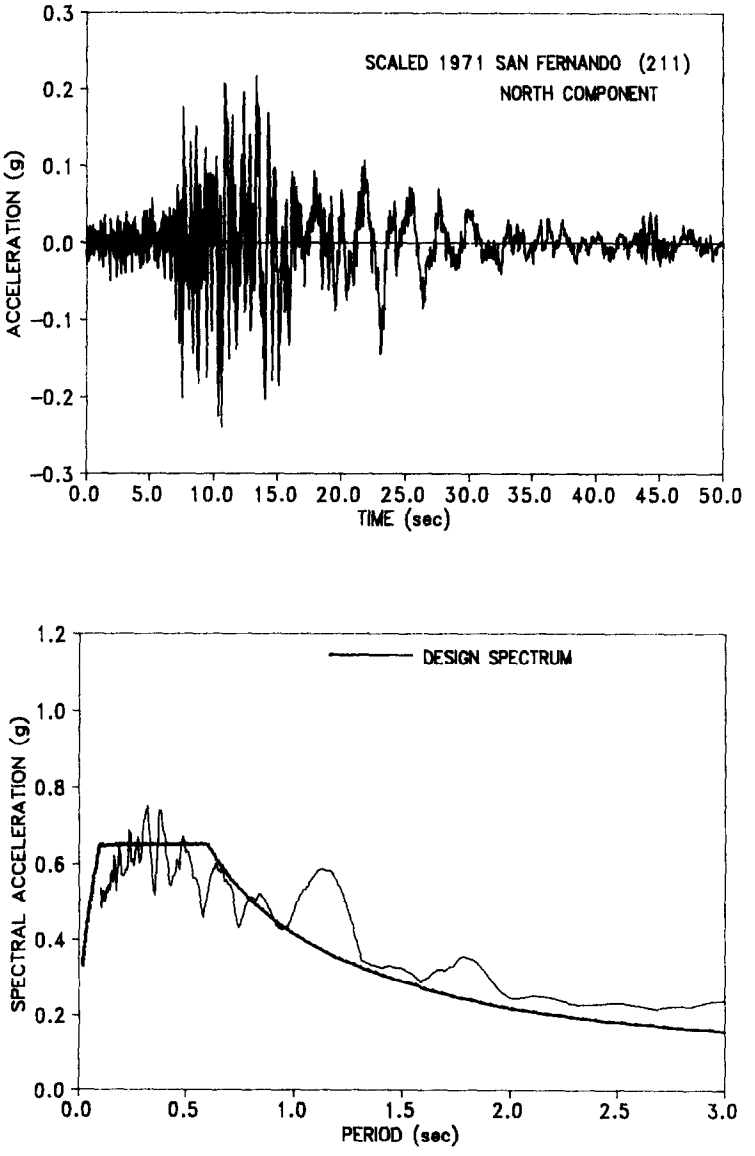

Fig. 6. Acceleration record of input motion and site specific response spectrum.

Table 3. Maximum response of part III of isolated hospital complex

		Complex		Individual	
Direction of ground motion		X		X	
Response direction		X	Y	X	Y
(Structure shear)/(weight)		0.236	0.023	0.181	0.001
	6	0.284	0.044	0.228	0.003
Peak floor	5	0.261	0.038	0.206	0.002
acceleration	4	0.248	0.026	0.189	0.001
at C.M. (g)	3	0.233	0.022	0.186	0.001
	2	0.216	0.015	0.194	0.002
	1	0.205	0.012	0.197	0.001
	6	0.122	0.012	0.097	0.010
Peak interstory	5	0.128	0.013	0.102	0.011
drift ratio at	4	0.129	0.012	0.102	0.010
corner column (%)	3	0.126	0.013	0.098	0.009
	2	0.100	0.012	0.079	0.009
	1	0.050	0.005	0.039	0.003
Corner bearing	67	0.128	0.003	0.133	0.003
peak displacement	70	0.128	0.002	0.133	0.003
(m)	95	0.128	0.003	0.131	0.003
	98	0.128	0.002	0.131	0.003

Complex: Analysis of entire complex. Individual: Analysis of Part III alone.

a comparison of its spectrum to the site specific response spectrum. The motion was applied in the X direction of the complex. As shown in Fig. 5, part III is placed at considerable distance from the center of mass of the entire complex. Its corner columns are at a distance of 34.34 m from the center of mass. For this part, the application of excitation in the X direction represents the worst loading condition. When part III is analyzed alone, its center of mass coincides with its geometric center and the corner columns are at distance of 14.85 m away of the center of mass.

A summary of the response of part III when analyzed as part of the complex and when analyzed alone is presented in Table 3. The table includes the peak floor accelerations at the center of mass of each floor, the peak corner column drift ratio at all stories, the peak structural shear over superstructure weight ($W^*_{III} = 28.13$ MN) ratio and the peak corner bearing displacements. Figure 7 presents the computed time histories of the indicated response quantities. Bearing displacements in the two analyses are almost the same. However, floor accelerations, interstory drifts and the structural shear in part III are larger in the analysis of the entire complex than in the analysis of part III alone. The underestimation of these response quantities in the analysis of part III alone amounts to about 25% of the values calculated in the analysis of the entire complex. Such deviation is significant and demonstrates the importance of interaction between adjacent buildings supported by a common isolation system.

Next an attempt is made to explain the observed differences in the response of the part III when analyzed alone and when analyzed as part of the complex. Part III has large eccentricities between the center of resistance and the center of mass of each floor. These eccentricities are primarily along the X direction, in which they assume values of more than 10% of the building's long dimension. In the Y direction, eccentricities are almost negligible.

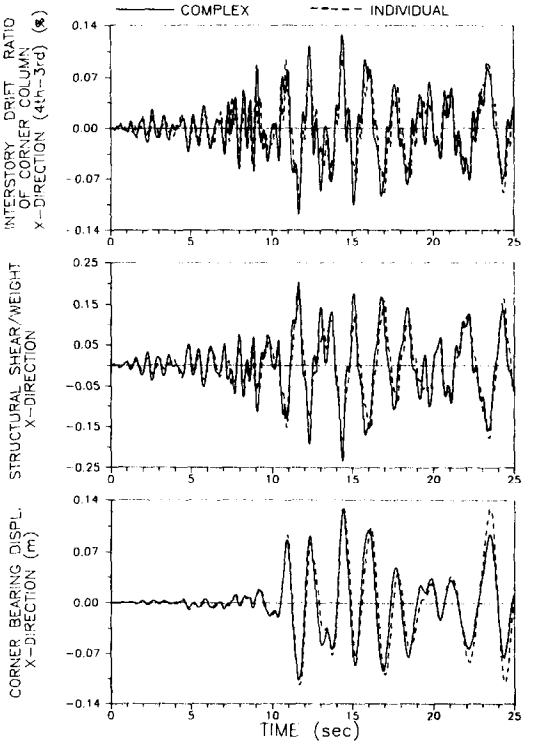

Fig. 7. Interstory drift ratio history of corner column (above bearing no. 67), structural shear history and base displacement history of corner bearing (bearing no. 67) of part III of isolated hospital complex.

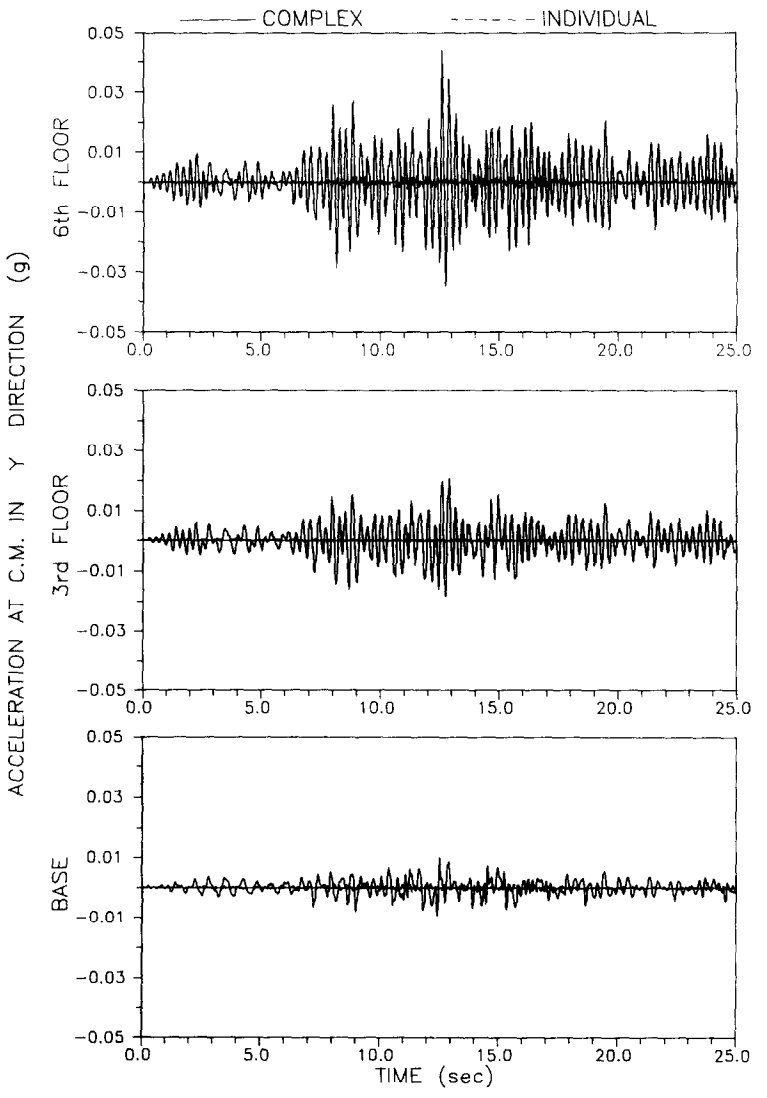

Fig. 8. Acceleration response in Y direction of part III of isolated hospital complex.

When part III is analyzed alone and excitation is applied in the X direction (see Fig. 5), the isolated part responds primarily in the X direction with insignificant motion in the Y direction. This is due to the almost zero eccentricities in the Y direction. When part III is analyzed as part of the complex and excitation is applied in X direction (see Fig. 5), the rotation of the T-shaped common basemat introduces a sizeable motion in the Y direction of part III. This is caused by the significant distance of the center of mass of part III from the center of mass of the common basemat which is 19.64 m. Figure 8 shows the distribution of acceleration with height in the Y direction of part III. When part III is analyzed alone, this acceleration is almost zero. When part III is analyzed as part of the complex, this acceleration reaches values of about 15% of the acceleration in X direction (see also results of Table 3). The acceleration that develops in the Y direction, when coupled with the sizable eccentricities in that direction, results in substantial rotation of the part with accordingly more floor acceleration and interstory drift.

CONCLUSIONS

The development of an analytical model for analyzing multiple building base-isolated structures has been presented. The accuracy of the analytical model has been verified. It was shown, by way of a case study, that the response of the combined system of several buildings on a common isolation system can be significantly different than that of individual buildings with individual isolation systems. The reason for this is that the torsional characteristics of the combined system can be significantly different than that of the individual system.

Acknowledgments—Financial support for the project has been provided by the National Center for Earthquake Engineering Research, contract No. 902101 and the National Science Foundation, grant No. BCS 8857080.

REFERENCES

1. J. M. Kelly, Aseismic base isolation: review and bibliography. *Soil Dyn. Earthquake Engng* **5**, 202–217 (1986).
2. J. M. Kelly, Base isolation in Japan, 1988. Report No. UBC/EERC-88/20, Earthquake Engineering Research Center, University of California, Berkeley, CA (1988).
3. I. G. Buckle and R. L. Mayes, Seismic isolation: history, application, and performance—A world overview. *Earthquake Spectra* **6**, 161–202 (1990).
4. M. C. Constantinou, A. Kartoum, A. M. Reinhorn and P. Bradford, Experimental and theoretical study of a sliding isolation system for bridges. Report No.-91-0027, National Center for Earthquake Engineering Research, State University of New York, Buffalo, NY (1991).
5. International Conference of Building Officials, Uniform building code, earthquake regulations for seismic isolated structures. Whittier, CA (1991).
6. A. M. Kannan and G. H. Powell, DRAIN-2D a general purpose computer program for dynamic analysis of inelastic plane structures with users guide. Report No. UCB/EERC-73/22, Earthquake Engineering Research Center, University of California, Berkeley, California (1975).
7. D. P. Mondkar and G. H. Powell, ANSR-General purpose program for analysis of nonlinear structural response. Report No. UCB/EERC-75/37, Earthquake Engineering Research Center, University of California, Berkeley, CA (1975).
8. D. Way and V. Jeng, NPAD—A computer program for the analysis of base-isolated structures. *ASME Pressure Vessels and Piping Conf.*, PVP-Vol. 147, Pittsburgh, pp. 65–69 (1988).
9. S. Nagarajaiah, A. M. Reinhorn and M. C. Constantinou, Nonlinear dynamic analysis of 3-D base-isolated structures. *J. Struct. Engng, ASCE* **117**, 2035–2054 (1991).
10. S. Nagarajaiah, A. M. Reinhorn and M. C. Constantinou, Nonlinear dynamic analysis of three dimensional base-isolated structures (3D-BASIS). Report No. NCEER-91-0005, National Center for Earthquake Engineering Research, State University of New York, Buffalo, NY (1989).
11. P. C. Tsopelas, S. Nagarajaiah, M. C. Constantinou and A. M. Reinhorn, 3D-BASIS-M: Nonlinear dynamic analysis of multiple building base-isolated structures. Report No. NCEER-91-0014, National Center for Earthquake Engineering Research, State University of New York, Buffalo, NY (1991).
12. E. L. Wilson, J. P. Hollings and H. H. Dovey, ETABS—Three dimensional analysis of building systems. Report No. UCB/EERC-75/13, Earthquake Engineering Research Center, University of California, Berkeley, CA (1975).
13. A. Yasaka, K. Mizukoshi, M. Izuka, Y. Takenaka, S. Maeda and N. Fujimoto, Biaxial hysteresis model for base isolation devices. *Summaries of Technical Papers of Annual Meeting—Architectural Institute of Japan* **1**, 395–400 (1988).
14. N. Mostaghel and M. Khodaverdian, Seismic response of structures supported on R-FBI system. *Earthquake Engng Struct. Dyn.* **16**, 839–854 (1988).
15. L. Su, G. Ahmadi and I. G. Tadjbakhsh, A comparative study of performance of various base isolation systems, Part I: Shear beam structures. *Earthquake Engng Struct. Dyn.* **18**, 11–32 (1989).
16. M. C. Constantinou, A. Mokha and A. M. Reinhorn, Teflon bearings in base isolation II: Modeling. *J. Struct. Engng, ASCE* **116**, 455–474 (1990).
17. Y. J. Park, Y. K. Wen and A. H. S. Ang, Random vibration of hysteretic systems under bidirectional ground motions. *Earthquake Engng Struct. Dyn.* **14**, 543–557 (1985).
18. A. Mokha, M. C. Constantinou and A. M. Reinhorn, Teflon bearings in base isolation I: Testing. *J. Struct. Engng, ASCE* **116**, 438–454 (1990).
19. A. Mokha, M. C. Constantinou and A. M. Reinhorn, Verification of friction model of Teflon bearings under triaxial load. *J. Struct. Engng, ASCE* **119**, 240–261 (1993).
20. N. M. Newmark, A method of computation for structural dynamics. *J. Engng Mech. Div., ASCE* **85**(EM3), 67–94 (1959).
21. H. H. Rosenbrock, Some general implicit processes for the numerical solution of differential equations. *Computer Jnl* **18**, 50–64 (1964).
22. Dynamic Isolation Systems, Inc. Seismic base isolation using lead–rubber bearings. Berkeley, CA (1983).